Journal of Materials Chemistry A

PAPER

View Article Online
View Journal | View Issue

Cite this: J. Mater. Chem. A, 2015, 3, 6440

CO_2 capture by dry alkanolamines and an efficient microwave regeneration process†

J. Yang,[a] H. Y. Tan,[a] Q. X. Low,[a] B. P. Binks*[b] and J. M. Chin*[ab]

Received 18th November 2014
Accepted 16th February 2015

DOI: 10.1039/c4ta06273f

www.rsc.org/MaterialsA

Removal of acidic gases such as H_2S and CO_2 is performed during the purification of raw natural gas, most commonly using amine gas treatment. However, this industrially entrenched method is limited by significant shortcomings including low operational capture efficiency, amine pipeline corrosion and a large energy penalty due to the sorbent regeneration process. To address these shortcomings, we have studied the use of perfluorinated silica-stabilized dry alkanolamines (DA_f) for CO_2 capture. Due to their micronized liquid domains, DA_f display high operational CO_2 capture efficiency. Further, to minimize energy requirements for sorbent regeneration, microwave-assisted regeneration of the spent DA_f sorbent was also studied and shown to decrease the energy requirements by about ten times. In contrast to very recent work, our results show that the use of DA_f exhibits extraordinary recyclability, with a negligible decrease in absorption capacity over at least ten absorption–regeneration cycles, indicating the potential of this material for gas treatment applications.

Introduction

Carbon dioxide capture is crucial not only for mitigating greenhouse gas emissions but also for natural gas processing.[1–4] The recent United States shale gas boom has precipitated an increase in the production of natural gas, making the need for effective CO_2 capture technologies more pressing than ever.[5] Examples of solid sorbents for CO_2 capture include metal–organic frameworks,[6–8] porous polymers[9–12] and zeolites.[13] Such sorbents have the advantage of a high surface area to accelerate CO_2 uptake.[14] Nevertheless, liquid sorbents, which often require agitation to achieve high gas–liquid interfacial areas, are still predominant in industrial processes. In fact, amongst various CO_2 capture technologies, the most established is amine gas treatment, which relies on the use of alkanolamines to separate acidic gases such as H_2S and CO_2 from raw natural gas.[15]

Despite amine-based gas sweetening being an already well-established industrial process, it faces multiple shortcomings including low operational CO_2 capture efficiency, amine corrosivity and a significant energy penalty due to the sorbent regeneration process.[1,16] Although primary and secondary alkanolamines react with CO_2 in a 2 : 1 mole ratio to form their corresponding carbamates with a theoretical CO_2 absorption capacity of 50 mol% (Scheme 1),[17–19] industrial systems utilizing alkanolamines typically only operate at 15 to 30 mol% capture efficiency.[20] In addition, the high viscosity and corrosivity of alkanolamines necessitate their dilution with water to approximately 30 wt% of amines.[6] This leads to an associated energy penalty during sorbent regeneration, whereby CO_2-loaded alkanolamine sorbents are heated to regenerate the amines, since the additional water content increases the overall heat capacity of the sorbent. To address this problem, researchers have turned to utilizing ionic liquid–alkanolamine blends[21] or to amine-functionalized porous solids for CO_2 capture.[22–24]

Dawson *et al.* recently reported an alternative approach whereby they used hydrophobic silica-stabilized dry alkanolamines (DA_h) for CO_2 capture.[25] However, the DA_h exhibited low recyclability and substantial sorbent loss during regeneration, as well as significantly decreased CO_2 uptake after the first cycle. Nevertheless, this approach circumvents the need for dilution of the sorbent with water, thereby decreasing the energy penalty incurred during sorbent regeneration. Amine-related corrosion problems are also potentially reduced because the amine is isolated by the silica particles from pipelines.

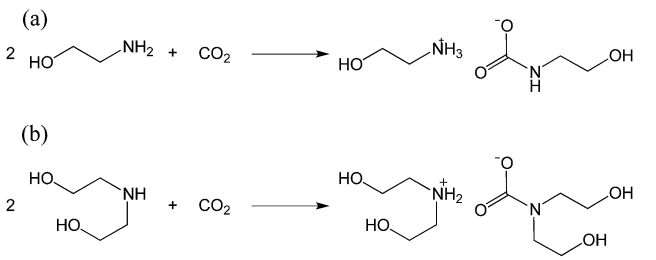

Scheme 1 Reaction of (a) monoethanolamine (MEA) and (b) diethanolamine (DEA) with CO_2 to form the corresponding carbamate salts.

[a]Institute of Materials Research and Engineering, Agency for Science Technology and Research, 3 Research Link, Singapore 117602, Singapore. E-mail: j.chin@hull.ac.uk
[b]Surfactant & Colloid Group, Department of Chemistry, University of Hull, HU6 7RX, UK. E-mail: b.p.binks@hull.ac.uk

† Electronic supplementary information (ESI) available: Detailed experimental procedures, ESI Fig. S1–S4 and ESI Tables S1–S3. See DOI: 10.1039/c4ta06273f

We herein report the use of dry, undiluted alkanolamines for CO_2 capture whereby instead of hydrocarbon-functionalized, hydrophobic fumed silica, perfluoroalkyl-functionalized oleophobic fumed silica was utilized for dry alkanolamine, DA, formation. These findings were previously outlined in our patent filed in May 2013,[26] prior to the work being reported by Dawson *et al.* We refer to this DA as DA_f. In contrast to the findings by Dawson *et al.*,[25] we found that DA_f showed excellent recyclability and stability. Studies were conducted on monoethanolamine (MEA) and diethanolamine (DEA) due to their widespread industrial usage. Furthermore, a novel method using microwave-assisted heating for DA_f regeneration was also investigated as an energy-efficient alternative to the conventional (convective and conductive heating) regeneration method.

DAs are powdered materials and can be thought of as inverted foams, *i.e.* liquid droplets dispersed in air, whereby microscopic liquid droplets stabilized by nanoparticles form the dispersed phase and air is the continuous matrix (Fig. 1). They appear as a free-flowing powder and are analogous in form to dry water (DW) which has received significant attention in recent years.[27–31]

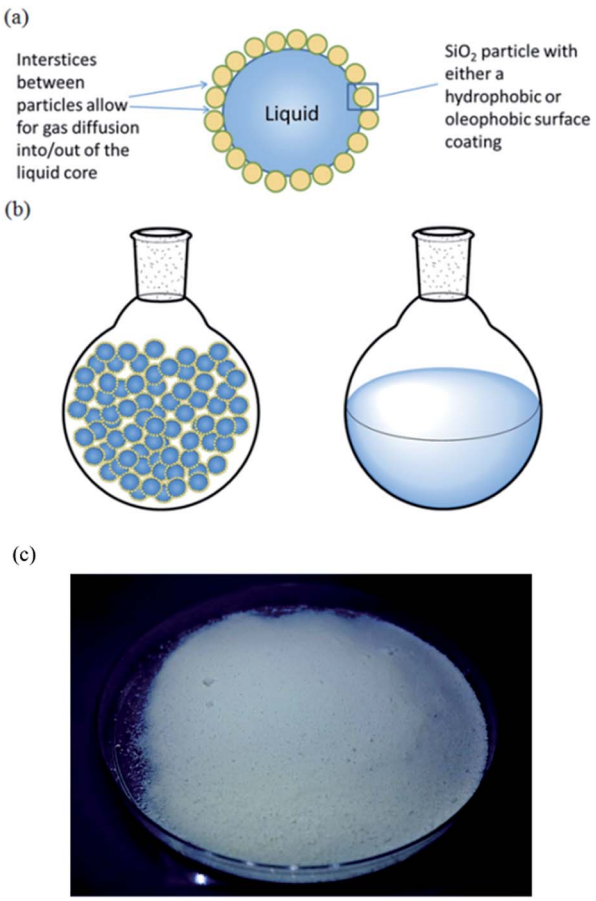

Fig. 1 (a) Sketch of a liquid droplet in air encapsulated by particles of low surface energy. Since the particles form a porous shell on the surface of the liquid, there is rapid diffusion of gases into and out of the liquid through the particle interstices. (b) Sketch of a dry liquid (left) and bulk liquid (right) in round-bottomed flasks. (c) Photograph of the DA_f powder containing DEA.

For dry liquid formation to occur, the stabilizing particles must be hydrophobic towards the encapsulated liquid, otherwise a foam or paste may ensue.[27] Generally, for a flat surface to be hydrophobic towards a liquid (contact angle > 90°), the solid surface tension γ_S must be $\gamma_S \ll \gamma_L/4$, where γ_L is the surface tension of the liquid.[32] It has recently been demonstrated that the formation of dry oils with liquids of decreasing surface tension requires the use of nanoparticles with increasing degrees of fluorination on their surfaces.[33] Based on the surface tensions of MEA and DEA (Table S1†), it can be deduced that oleophobic perfluoroalkyl-functionalized nanoparticles are preferable over oleophilic hydrocarbon-functionalized nanoparticles for stabilization of DAs (Fig. S1†).

Experimental

Materials

All materials were purchased from commercial sources and used as received. 1*H*,1*H*,2*H*,2*H*-Perfluorooctyltriethoxysilane (purity 97%) was purchased from Fluorochem. Ethanolamine (purity 98%), diethanolamine (purity 98%) and hydrophilic fumed silica powder with an average particle size (aggregate) of 0.2–0.3 μm (product number S5505) were purchased from Sigma Aldrich. Ethanol (purity 99%) was purchased from International Scientific. Aqueous ammonia (28%) was purchased from Malayan Acid Works. Compressed CO_2 (purity 99.8%) was purchased from Singapore Oxygen Air Liquide.

Methods

Synthesis of perfluoroalkyl-functionalized oleophobic SiO_2 nanoparticles. 10 g of fumed SiO_2 was added to a well-mixed solution of 220 mL ethanol, 11 mL of 28% aqueous NH_3 and 2 mL of 1*H*,1*H*,2*H*,2*H*-perfluorooctyltriethoxysilane, which was then homogenized (using an IKA T18 basic Ultra Turrax digital homogenizer) for 30 min until a homogeneous suspension was obtained. The resulting dispersion was stirred at 400 ± 50 rpm at room temperature overnight, after which the dispersion was heated on a hot plate to evaporate the solvents and subsequently dried in an oven at 80 °C for 1–2 days to collect the dry perfluorinated silica powder. Thermogravimetric analysis (TGA) was performed using a TGA Q500 v6.7 Build 203 instrument, from room temperature to 800 °C at a rate of 20 °C min^{-1} with 40 mL min^{-1} of nitrogen gas as the balance gas and 60 mL min^{-1} of air as the sample gas. TGA of perfluorinated silica *versus* unmodified fumed silica particles showed that the perfluorocarbon groups comprised approximately 35 wt% of the functionalized silica (Fig. S2†). Dynamic Light Scattering (DLS) studies were performed with a Brookhaven ZetaPlus Zeta Potential Analyzer to determine the size distribution of unmodified fumed silica particles *versus* perfluorinated fumed silica particles after dispersing them in ethanol. DLS studies showed that the average aggregate size of perfluorinated silica particles was smaller than that of unmodified fumed silica particles (282 nm *vs.* 367 nm, see Table S2†).

Preparation of dry alkanolamines. 5 g of perfluorinated SiO_2 nanoparticles was placed in a plastic beaker while 5 mL of the selected alkanolamine (pre-heated for 1 h at 100 °C to minimize the water content) was slowly added into the beaker and blended with the particles using a simple coffee whisk (Fig. S3a†) at a rate of 500–1800 rpm for 1 min or until the formation of a free-flowing powder.

Absorption of CO_2 into bulk or dry alkanolamines. The reaction was performed at room temperature and pressure. 5 mL of alkanolamine or approximately 10 g of DA_f powder (containing 5 mL of alkanolamine) was added into a round-bottomed flask placed in a water bath to modulate the heating effects arising from the exothermic nature of the reaction. CO_2 gas was bubbled at a flow rate of 500 ± 50 mL min^{-1} through the flask with the outlet connected to a gas bubbler until the absorption profile plateaued. At short time intervals of 30 s or 1 min, the flask was taken out of the water bath, dried and weighed on a weighing balance to record the increase in mass. The maximum CO_2 uptake by alkanolamines (in the absence of water) was calculated by assuming a reaction mole ratio of 2 : 1 alkanolamine to CO_2.

Regeneration of sorbents by conventional hotplate heating. The CO_2-loaded alkanolamine or DA_f powder was regenerated by bubbling argon gas at a flow rate of 500 ± 50 mL min^{-1} through the sorbent while the flask was heated in an oil bath at 120 °C to release the absorbed CO_2. The flask was equipped with a reflux condenser maintained at 15 °C to minimize the evaporative loss of the sorbents and the outlet was connected to a gas bubbler.

Regeneration of sorbents by dielectric heating. The CO_2-loaded DA_f powder was added into an open Teflon cup. The cup was placed in a holder and subsequently placed in a programmable microwave synthesizer at 2.45 GHz. The maximum power of the synthesizer was set at 500 W. No purge gas was used. To maintain the stripping temperature of 120 °C, a thermocouple was inserted into a separate Teflon cup containing unloaded-sorbent which provided feedback to the software to control the microwave power. In addition, stirring of the sample within the cup was carried out as part of the microwave heating process. The microwave synthesizer was used to heat the CO_2-loaded sorbent at 120 °C for approximately 1 h until no further mass loss occurred, after which time the cup was removed and weighed. The decrease in weight was attributed to the CO_2 loss (typical mass decrease for diethanolamine: 0.08–0.1 g g^{-1} DA_f or 0.16–0.2 g g^{-1} bulk DEA).

Results and discussion

Brunauer–Emmett–Teller (BET) analysis performed on perfluorinated SiO_2 particles showed that CO_2 adsorption on these particles at room temperature was negligible (Fig. 2), because 1 g of perfluorinated SiO_2 nanoparticles absorbed approximately 6 mg of CO_2 at atmospheric pressure while 1 g of DA_f (containing 0.48 g of perfluorinated silica) absorbed approximately 100 mg of CO_2. Of this 100 mg, about 3% is attributed to adsorption by silica. Hence, the mass increase is largely due to CO_2 uptake by the alkanolamine.

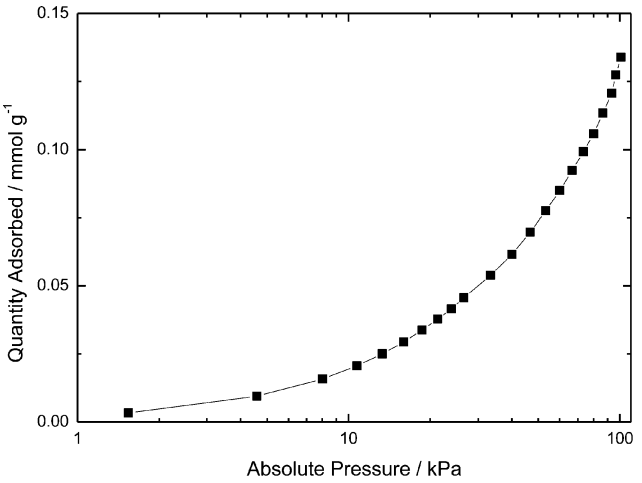

Fig. 2 Isothermal CO_2 adsorption at 22 °C by perfluorinated SiO_2 nanoparticles showing negligible CO_2 uptake (0.135 mmol g^{-1} at 100 kPa).

Carbon dioxide absorption results for both DA_f and bulk liquid are shown in Fig. 3. The theoretical maximum alkanolamine CO_2 uptake (in the absence of water) was calculated by assuming a reaction mole ratio of 2 : 1 alkanolamine to CO_2. Hence, 1 g MEA theoretically absorbs about 0.36 g CO_2 at the maximum, and 1 g DEA theoretically absorbs 0.21 g CO_2. As shown in Fig. 3, CO_2 absorption by dry and bulk MEA in the first 10 min of CO_2 exposure reached 98 and 60 wt% of the theoretical maximum absorption, respectively. Similarly, dry and bulk DEA achieved about 90 and 35 wt% of the theoretical maximum within 20 min. Mass changes due to the replacement of air in the reaction vessel headspace with CO_2 were taken into account in the calculations.

For both amines, the DA_f showed significantly higher CO_2 absorption than their corresponding bulk liquid counterparts (Fig. 3). The lower absolute absorption of the bulk amines is due to mass transport effects arising from the large increase in the liquid viscosity caused by carbamate salt formation, which was verified by measuring the viscosities of the alkanolamine liquids before and after CO_2 absorption (Table S3†). The effect of viscosity of a liquid on the mass transfer kinetics is described by the Stokes–Einstein equation:[34]

$$D_{ij} = \frac{kT}{n_{SE}\pi\eta_j R_i}\left[\frac{R_j}{R_i}\right] \quad (1)$$

In this equation, D_{ij} is the diffusion coefficient of solute i in pure solvent j, k is the Boltzmann constant, T is the temperature, n_{SE} is the Stokes–Einstein number, η_j is the solvent viscosity, R_i is the radius of the solute molecule and R_j is the radius of the solvent molecule. According to eqn (1), the diffusion coefficient of CO_2 gas in the amine sorbent decreases with increasing solvent viscosity. Further, given that the system studied is stationary and unagitated, the increased viscosity also significantly affects the replenishing of the unreacted amine near the gas–liquid interface, which is dependent upon the

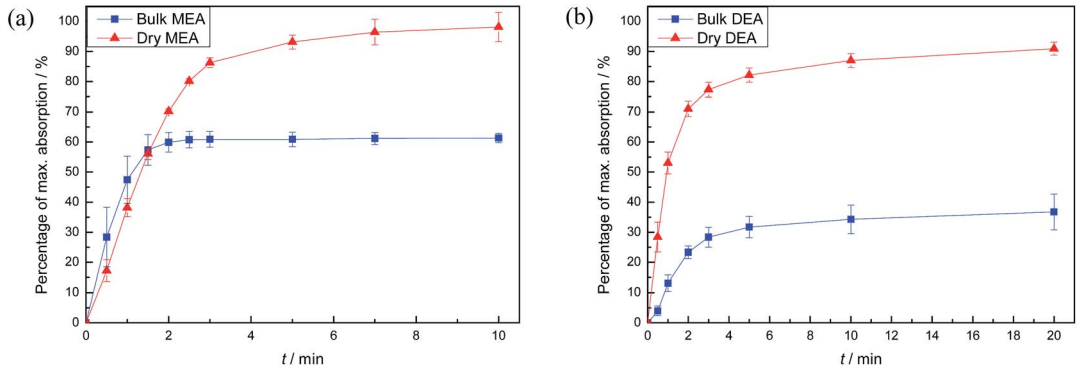

Fig. 3 Results of the absorption profile of CO_2 into bulk alkanolamine or DA_f for (a) MEA and (b) DEA at room temperature and pressure.

movement of alkanolamine molecules towards the interface *via* convection currents or diffusion.

However, due to the small domain sizes within DA_f (approximate diameter of a microscopic liquid marble is 80 ± 30 μm, as measured by cryo-SEM), the required distance of CO_2 diffusion within the droplets to contact the unreacted alkanolamine is significantly less than for the bulk liquid. This helps to explain why the DA_f achieve a much larger gas absorption relative to the theoretical capacity within the timeframe of the experiment than do the bulk amines. In addition, the reason for the slightly higher absorption capacity of dry MEA compared to dry DEA is due to the inherently lower viscosity of the former compared to the latter.

Based on the work of Wang *et al.*,[31] who postulated that the higher methane gas hydrate formation rate in dry *versus* bulk water was due to the higher surface area to volume ratio in dry water, and taking the view that the rate of gas uptake is dependent upon the gas–liquid interfacial area, we expect that the CO_2 absorption rate by DA_f would follow a similar trend (estimated surface area to volume ratio in DA_f is 75 000 m^{-1} based on the volume of alkanolamine present). Nevertheless, the gas–liquid interfacial area of the microscopic liquid droplets is reduced by the presence of the silica shell around each droplet; CO_2 must diffuse across this porous shell to react with the encapsulated alkanolamines.

Our CO_2 uptake studies showed that for MEA, the absorption rate by the bulk liquid in the first minute was faster than that by dry MEA (Fig. S4†). This is presumably because the lower liquid viscosity of MEA compared with DEA means that CO_2 mass transfer effects do not outweigh the effect of the silica barrier initially. However, as carbamate formation proceeds, the viscosity of the liquid mixture increases (Table S3†), and mass transfer effects become more important. The rate of CO_2 uptake therefore becomes faster for dry over bulk MEA. For DEA, dry DEA exhibits faster CO_2 absorption than bulk DEA throughout the entire absorption cycle (Fig. S4†), because the mass transfer rate in the more viscous DEA liquid was much slower and hence the effect of higher surface area to volume ratio of dry DEA was more prominent.

Since the carbamate salts decompose in the temperature range of 100–150 °C,[35,36] the CO_2-loaded bulk alkanolamines were heated to 120 °C to release the absorbed CO_2 gas and regenerate the alkanolamines. The decrease in mass was attributed to both CO_2 and H_2O release, which was verified by thermogravimetric mass spectroscopy (TG-MS) analysis (see Fig. 4).

For each sample of bulk alkanolamine and DA_f, three cycles of absorption and desorption of CO_2 were performed (Fig. 5). As shown in Fig. 5, DEA appears to be more recyclable than MEA, with a negligible change in CO_2 uptake capacity over three cycles. This is because secondary amines like DEA form weaker bonds with CO_2 than primary amines like MEA, allowing for easier regeneration of the free amines.[37] This is supported by the findings of McCann *et al.*, where the enthalpy of carbamate formation for MEA and DEA was found to be −29.7 kJ mol^{-1} and −23.7 kJ mol^{-1}, respectively.[38] Moreover, MEA has a lower boiling point than DEA (170 °C *vs.* 271 °C) and a much higher vapour pressure, leading to a greater degree of sorbent loss per cycle.

As heating is essential for the sorbent regeneration process, it is imperative to maximize the heat transfer efficiency within the amine sorbents. This is dependent on the three main mechanisms of heat transfer, namely conduction, convection and radiation. In the case of DA_f, these three mechanisms happen to be hindered by the silica shell encasing the micronized alkanolamine droplets and the air pockets throughout the dry liquids. For heat transfer *via* conduction, fumed silica particles exhibit low thermal conductivity due to the nanoscale pores among them in their fractal arrangement,[39,40] causing the silica shell to block effective heat conduction from the heat source to the droplets. Importantly, many air pockets between the microscopic particle-coated liquid marbles in DA_f also limit heat conductivity. With regard to convection, the liquid in DA_f exists as dispersed microscopic droplets, thereby limiting convective heat transfer. As for radiative heat transfer, Taylan and Berberoglu have shown that the silica shell in dry water greatly attenuates infrared radiative heat transfer due to its high single-scattering albedo, *i.e.* a significantly larger proportion of heat radiation is scattered compared to that absorbed by the silica shell,[41] thus preventing infrared radiative heat transfer from the heat source to the droplets.

Since the three major forms of heat transfer are significantly inhibited for DA_f, we turned to microwave heating as an alternative method to improve the efficiency of heat transfer during

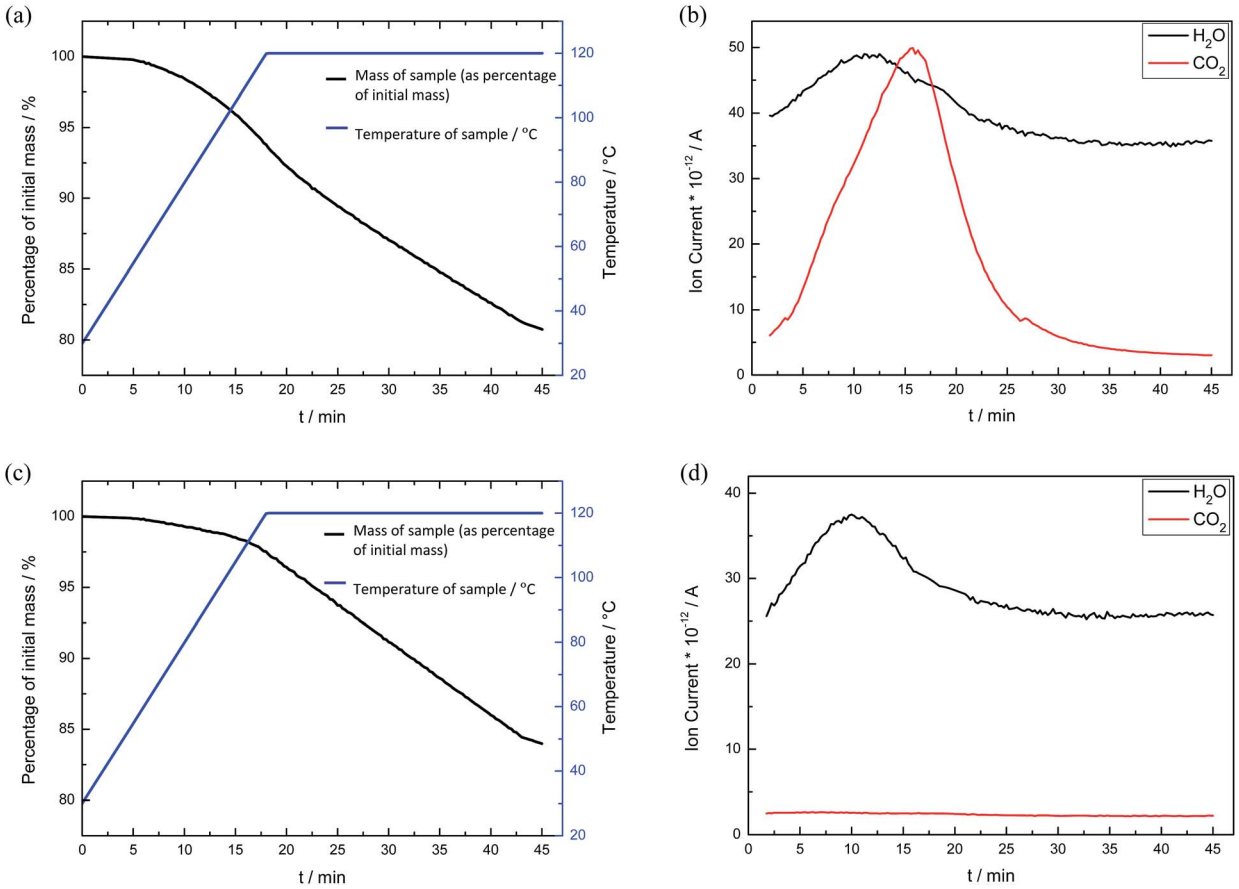

Fig. 4 (a and b) TG-MS graphs of CO_2-loaded bulk DEA, and (c and d) TG-MS graphs of bulk DEA without CO_2 loading. (a) The black line shows a decrease of 18.92% of the initial sample mass for CO_2-loaded bulk DEA with a concomitant increase in the sample temperature from 30 to 120 °C as depicted by the blue line, (b) graph corresponding to (a), depicting ion current detection of both CO_2 and H_2O. (c) The black line shows a decrease of 16.03% of the initial sample mass for bulk DEA, (d) graph corresponding to (c) depicting detection of only H_2O but not CO_2.

the regeneration process. This method is dependent on the ability of the irradiated material, *e.g.* a solvent, to absorb microwave energy and convert it to heat, which is quantified by a dielectric parameter called the loss factor tan δ. This loss factor is expressed as:[42]

$$\tan \delta = \frac{\varepsilon''}{\varepsilon'} \quad (2)$$

where ε'' is the dielectric loss, which is indicative of the efficiency with which electromagnetic radiation is converted into heat, and ε' is the dielectric constant describing the ability of molecules to be polarized by the electric field. A solvent with a high tan δ value of more than 0.5 is required for efficient microwave absorption. DEA, with a high tan δ value of ~0.6 at 2.45 GHz at 278 K can be rapidly heated to temperatures >100 °C within a minute when irradiated under microwave conditions.[43]

Owing to the higher recyclability of DEA over MEA, we chose to study DEA for microwave heating-based regeneration. Samples of approximately 10 g of dry DEA containing 5 mL of liquid DEA were loaded with CO_2 until the absorption plateaued, and the CO_2-loaded samples were subsequently heated in a programmable microwave synthesizer at 120 °C for approximately 1 h until no further mass loss occurred. To test the recyclability of the sorbent and confirm that the observed mass loss was correctly attributed to the CO_2 loss, 10 repeated cycles of CO_2 absorption and removal were carried out, as shown in Fig. 6. The level of CO_2 uptake by dry DEA was found to be stable over at least 10 cycles, showing an excellent recyclability of dry DEA. Similar regeneration results were obtained using a simple household microwave instrument, although the heating periods were limited to 10–20 s in order to avoid overheating.

Regeneration of DA_f *via* microwave heating was found to be more efficient than conventional hotplate heating under the same conditions (whereby no purge gas was used). Conventional hotplate heating took more than 3 h and consumed about 0.38 kW h per cycle on average. Microwave heating on the other hand took about 1 h and consumed about 0.034 kW h per cycle on average, which is less than 10% of the energy consumption by conventional hotplate heating.

Finally, the recyclability of the perfluorinated silica particles was investigated. Alkanolamines typically undergo degradation over multiple absorption and regeneration cycles after which they must be replaced.[44] Nevertheless, the perfluorinated silica particles could be separated from the amines by dispersion of

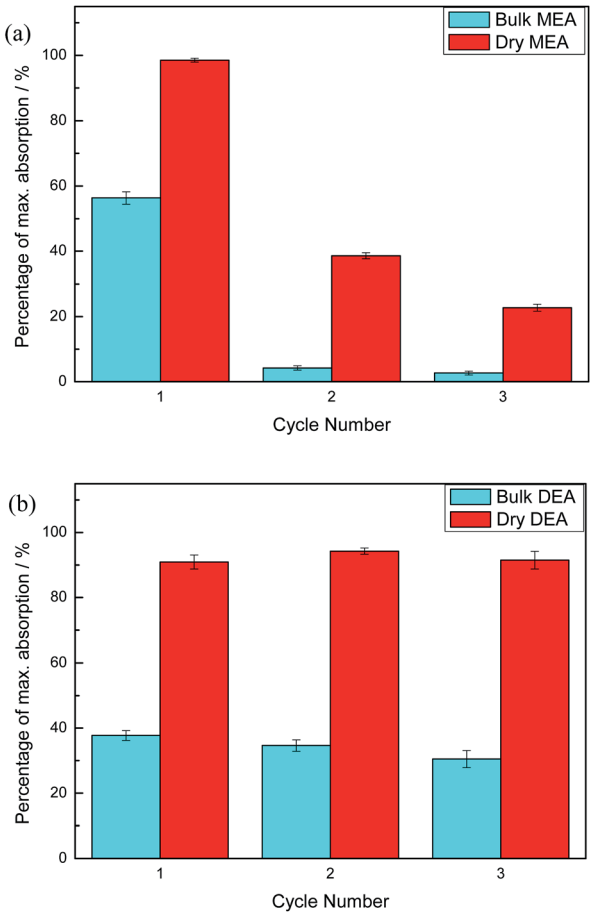

Fig. 5 Comparison of solvent recyclability of (a) bulk MEA *versus* dry MEA, whereby heating lasts for 2 h for each cycle of regeneration and (b) bulk DEA *versus* dry DEA, whereby heating lasts for 1 h for each cycle of regeneration.

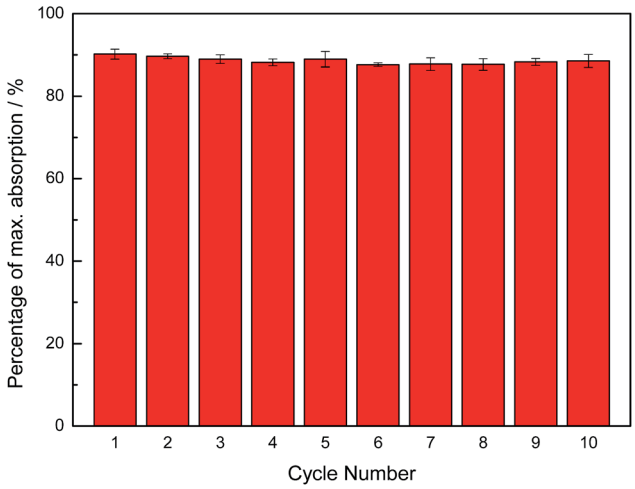

Fig. 6 Sorbent recyclability of dry DEA using dielectric heating (1 h per cycle) for regeneration, showing a negligible drop in absorption capacity over 10 cycles.

DA_f in ethanol and then centrifuged, and re-used in at least three subsequent batches of DA_f. This leads to significant cost-savings since only the alkanolamines need to be replaced.

Conclusions

In conclusion, the dry alkanolamines described herein demonstrate significantly enhanced performance with regard to CO_2 absorption capacity and sorbent recyclability. Furthermore, the novel dielectric heating technique for sorbent regeneration proposed here has proven to possess the benefits of reduced energy consumption and minimal use of purge gas. The perfluorinated silica particles can also be recycled and re-used to prepare DA_f with a negligible change in their wettability and overall quality for at least three cycles. Moreover, as suggested by the recent work of Dawson *et al.*,[25] the amine component of the DA_f is also isolated by the silica particles from pipelines and other corrosion sensitive materials, leading to further reduction in maintenance costs associated with the addition of corrosion inhibitors and repair of damage to pipelines. Last but not least, this novel method of using DA_f is not restricted to MEA and DEA; in principle any dry liquid can be formed provided that nanoparticles of appropriate surface energy are selected.[33] The implications are that this idea can be extended to other liquid CO_2 sorbents, possibly leading to a similar improvement in the absorption rate and capacity. However, there still exist several challenges for the application of DA_f industrially. Firstly, the powdery nature of DA_f will likely require significant changes in the current process technology and facilities specialized in handling liquid amine sorbents. Secondly, due to the nanoscale primary particle size of fumed silica, careful confinement of the powder needs to be put in place to prevent contamination in the outlet gas stream. Thirdly, stripper columns need to be modified to incorporate dielectric heating capabilities. Nevertheless, given the multiple advantages of utilizing DA_f for CO_2 absorption and desorption, we believe that they should still be considered promising candidates for practical applications in CO_2 capture.

Acknowledgements

JMC would like to acknowledge the Institute of Materials Research and Engineering, Agency for Science Technology and Research (A*STAR) for funding this work. The authors thank Mr Anthony Sinclair for the cryo-SEM analysis, Ms Sophie A. Darragh, Dr Michael R. Reithofer, Dr Tommy S. Horozov, Dr Robert A. Lewis and Dr R. McDonald for helpful discussions.

Notes and references

1 S. Anderson and R. Newell, *Annu. Rev. Environ. Resour.*, 2004, **29**, 109–142.
2 C. Yu, C. Huang and C. Tan, *Aerosol Air Qual. Res.*, 2012, **12**, 745–769.
3 D. M. D'Alessandro, B. Smit and J. R. Long, *Angew. Chem., Int. Ed.*, 2010, **49**, 6058–6082.

4 N. MacDowell, N. Florin, A. Buchard, J. Hallett, A. Galindo, G. Jackson, C. S. Adjiman, C. K. Williams, N. Shah and P. Fennell, *Energy Environ. Sci.*, 2010, **3**, 1645–1669.
5 H. D. Jacoby, F. M. O'Sullivan and S. Paltsev, *MIT Joint Program on the Science and Policy of Global Change*, 2011.
6 Z. Zhang, Z. Yao, S. Xiang and B. Chen, *Energy Environ. Sci.*, 2014, **7**, 2868–2899.
7 P. Nugent, Y. Belmabkhout, S. D. Burd, A. J. Cairns, R. Luebke, K. Forrest, T. Pham, S. Ma, B. Space, L. Wojtas, M. Eddaoudi and M. J. Zaworotko, *Nature*, 2013, **495**, 80–84.
8 W. R. Lee, S. Y. Hwang, D. W. Ryu, K. S. Lim, S. S. Han, D. Moon, J. Choi and C. S. Hong, *Energy Environ. Sci.*, 2014, **7**, 744–751.
9 H. A. Patel, S. H. Je, J. Park, D. P. Chen, Y. Jung, C. T. Yavuz and A. Coskun, *Nat. Commun.*, 2013, **4**, 1357.
10 W. Lu, J. P. Sculley, D. Yuan, R. Krishna, Z. Wei and H.-C. Zhou, *Angew. Chem., Int. Ed.*, 2012, **51**, 7480–7484.
11 H. Hea, W. Lia, M. Zhong, D. Konkolewicza, D. Wub, K. Yaccato, T. Rappold, G. Sugar, N. E. David and K. Matyjaszewski, *Energy Environ. Sci.*, 2013, **6**, 488–493.
12 H. He, M. Zhong, D. Konkolewicz, K. Yacatto, T. Rappold, G. Sugar, N. E. David, J. Gelb, N. Kotwal, A. Merkle and K. Matyjaszewski, *Adv. Funct. Mater.*, 2013, **23**, 4720–4728.
13 F. Sua and C. Lu, *Energy Environ. Sci.*, 2012, **5**, 9021–9027.
14 Q. Wang, J. Luo, Z. Zhong and A. Borgna, *Energy Environ. Sci.*, 2011, **4**, 42–55.
15 G. T. Rochelle, *Science*, 2009, **325**, 1652–1654.
16 Y. E. Kim, J. A. Lim, S. K. Jeong, Y. Yoon, S. T. Bae and S. C. Nam, *Bull. Korean Chem. Soc.*, 2013, **34**, 783–787.
17 S. S. Laddha and P. V. Danckwerts, *Chem. Eng. Sci.*, 1981, **36**, 479–482.
18 P. V. Danckwerts, *Chem. Eng. Sci.*, 1979, **34**, 443–446.
19 E. Sada, H. Kumazawa, Z. Q. Han and H. Matsuyama, *AIChE J.*, 1985, **31**, 1297–1303.
20 A. B. Rao and E. S. Rubin, *Environ. Sci. Technol.*, 2002, **36**, 4467–4475.
21 M. Hasib-ur-Rahman and F. Larachi, *Environ. Sci. Technol.*, 2012, **46**, 11443–11450.
22 C. Chen, J. Kim and W. Ahn, *Korean J. Chem. Eng.*, 2014, **3**, 1919–1934.
23 M. Pera-Titus, *Chem. Rev.*, 2014, **114**, 1413–1492.
24 K. Sumida, D. L. Rogow, J. A. Mason, T. M. McDonald, E. D. Bloch, Z. R. Herm, T. Bae and J. R. Long, *Chem. Rev.*, 2012, **112**, 724–781.
25 R. Dawson, L. A. Stevens, O. S. A. Williams, W. Wang, B. O. Carter, S. Sutton, T. C. Drage, F. Blanc, D. J. Adams and A. I. Cooper, *Energy Environ. Sci.*, 2014, **7**, 1786–1791.
26 Dry Liquids for Gas Absorption and Purification, J. M. Chin, S. W. Tay, J. W. Xu and A. Y. X. Tan, Assigned to Agency for Science, Technology and Research, Singapore, *SG. Pat.* 2013040316, 23 May 2013.
27 B. P. Binks and R. Murakami, *Nat. Mater.*, 2006, **5**, 865–869.
28 B. O. Carter, D. J. Adams and A. I. Cooper, *Green Chem.*, 2010, **12**, 783–785.
29 L. Forny, K. Saleh, R. Denoyel and I. Pezron, *Langmuir*, 2009, **26**, 2333–2338.
30 G. Hu, Y. Ye, C. Liu, Q. Meng, J. Zhang and S. Diao, *Fuel Process. Technol.*, 2011, **92**, 1617–1622.
31 W. Wang, C. L. Bray, D. J. Adams and A. I. Cooper, *J. Am. Chem. Soc.*, 2008, **130**, 11608–11609.
32 K. Tsujii, T. Yamamoto, T. Onda and S. Shibuichi, *J. Colloid Interface Sci.*, 1998, **208**, 1011–1012.
33 B. P. Binks, T. Sekine and A. T. Tyowua, *Soft Matter*, 2014, **10**, 578–589.
34 M. J. W. Frank, J. A. M. Kuipers and W. P. M. van Swaaij, *J. Chem. Eng. Data*, 1996, **41**, 297–302.
35 P. Zhang, Y. Shi, J. Wei, W. Zhao and Q. Ye, *J. Environ. Sci.*, 2008, **20**, 39–44.
36 D. Bonenfant, M. Mimeault and R. Hausler, *Ind. Eng. Chem. Res.*, 2003, **42**, 3179–3184.
37 W. Lu, J. P. Sculley, D. Yuan, R. Krishna, Z. Wei and H. Zhou, *Angew. Chem., Int. Ed.*, 2012, **51**, 7480–7484.
38 N. McCann, M. Maeder and H. Hasse, *J. Chem. Thermodyn.*, 2011, **43**, 664–669.
39 H. Abe, I. Abe, K. Sato and M. Naito, *J. Am. Ceram. Soc.*, 2005, **88**, 1359–1361.
40 T. Kashiwagi, J. W. Gilman, K. M. Butler, R. H. Harris and J. R. Shields, *Fire Mater.*, 2001, **24**, 277–289.
41 O. Taylan and H. Berberoglu, *J. Quant. Spectrosc. Radiat. Transfer*, 2013, **120**, 104–113.
42 C. O. Kappe, *Angew. Chem., Int. Ed.*, 2004, **43**, 6250–6284.
43 A. V. Patil and V. P. Pawar, *J. Mol. Liq.*, 2013, **188**, 1–4.
44 G. S. Goff and G. T. Rochelle, *Ind. Eng. Chem. Res.*, 2006, **45**, 2513–2521.

